

**RANGE ESTIMATION USING PHASE DIFFERENCE OF ARRIVAL  
TECHNIQUE**

**TITILOYE STEPHEN OYEDIRAN**

**UNIVERSITI TEKNOLOGI MALAYSIA**

## UNIVERSITI TEKNOLOGI MALAYSIA

**DECLARATION OF THESIS / UNDERGRADUATE PROJECT REPORT AND COPYRIGHT**Author's full name : **TITILOYE STEPHEN OYEDIRAN**Date of Birth : **24 OCTOBER 1967**Title : **RANGE ESTIMATION USING PHASE DIFFERENCE OF ARRIVAL TECHNIQUE**Academic Session: **2015/2016 – 1**

I declare that this thesis is classified as:

- CONFIDENTIAL** (Contains confidential information under the Official Secret Act 1972)\*
- RESTRICTED** (Contains restricted information as specified by the organization where research was done)\*
- OPEN ACCESS** I agree that my thesis to be published as online open access (full text)

I acknowledged that Universiti Teknologi Malaysia reserves the right as follows:

1. The thesis is the property of Universiti Teknologi Malaysia
2. The Library of Universiti Teknologi Malaysia has the right to make copies for the purpose of research only.
3. The Library has the right to make copies of the thesis for academic exchange.

Certified by:

\_\_\_\_\_  
SIGNATURE\_\_\_\_\_  
201409M10224  
(NEW IC NO./PASSPORT)

Date: 31 DECEMBER 2015

\_\_\_\_\_  
SIGNATURE OF SUPERVISOR\_\_\_\_\_  
Dr. Kamaludin Mohamad Yusof  
NAME OF SUPERVISOR

Date: 31 DECEMBER 2015

**NOTES:** \* If the thesis is **CONFIDENTIAL** or **RESTRICTED**, please attach with the letter from the organization with period and reasons for confidentiality or restriction.

“I hereby declare that I have read this project report and in my opinion this project report is sufficient in terms of scope and quality for the award of the degree of master of Engineering (Electronics & Telecommunication)”

Signature : .....  
Name of Supervisor : DR. KAMALUDIN MOHAMMAD YUSOF  
Date : 31 December 2015

**BAHAGIAN A – Pengesahan Kerjasama\***

Adalah disahkan bahawa projek penyelidikan tesis ini telah dilaksanakan melalui kerjasama antara \_\_\_\_\_ dengan \_\_\_\_\_

Disahkan oleh:

Tandatangan : ..... Tarikh : .....

Nama : .....

Jawatan : .....  
(Cop rasmi)

*\* Jika penyediaan tesis/projek melibatkan kerjasama.*

---

---

**BAHAGIAN B – Untuk Kegunaan Pejabat Sekolah Pengajian Siswazah**

Tesis ini telah diperiksa dan diakui oleh:

Nama dan Alamat Pemeriksa Luar : \_\_\_\_\_  
\_\_\_\_\_

Nama dan Alamat Pemeriksa Dalam : \_\_\_\_\_  
\_\_\_\_\_

Nama Penyelia lain (jika ada) : \_\_\_\_\_  
\_\_\_\_\_

Disahkan oleh Timbalan Pendaftar di Sekolah Pengajian Siswazah:

Tandatangan : ..... Tarikh : .....

Nama : .....

RANGE ESTIMATION USING PHASE DIFFERENCE OF ARRIVAL  
TECHNIQUE

TITILOYE STEPHEN OYEDIRAN

A project report submitted in partial fulfillment of the  
requirements for the award of the degree of  
Masters of Engineering (Electronics & Telecommunication)

Faculty of Electrical Engineering  
Universiti Teknologi Malaysia

DECEMBER 2015

“I declare that this project report entitled “*Range Estimation Using Phase Difference of Arrival Technique*” is the result of my own research except as cited in the references. The project report has not been accepted for any degree and is not concurrently submitted in candidature of any other degree.”

Signature : .....

Name : TITILOYE STEPHEN OYEDIRAN

Date : 31 December 2015

To my beloved wife, Engr. Mrs. Yetunde Titiloye – my Jewel of  
inestimable value

## ACKNOWLEDGEMENT

Unto the Lord be the glory, great things He hath done. I praise the Almighty God, the sustainer of my life. HIS love and mercy have seen me through this programme. May His name be exalted for ever, Amen.

I really appreciate my project supervisor, *Dr. Kamaludin Mohamad Yusof*, whose directives and academic acumen guided me properly. He's always there for me anytime.

My sincere heartfelt gratitude also goes to my Darling wife, *Engr. Mrs. Yetunde Titiloye* and my children, *Mofiyinfoluwa, Moromoluwa, Abigail, Adeola and Nicholas* for their tireless and unwavering support for me, ensuring that I succeed all the way. I appreciate them for bearing with me and for their understanding why I had to leave them to pursue this programme in a far country.

Thanks to Surv. Alamu E. O. of Surveying & Geoinformatics department, Mrs. Elizabeth Gata of Business Administration department and Mrs. Buhari of Science Laboratory department, whose financial support kick-started me on a sound note.

I say thank you all, God bless you.



## ABSTRACT

The principle of positioning is a technology of identification that enables object, people and/or assets to be tracked. This is basically to allow objects to be found for the purpose of rendering/obtaining services. Ranging technique therefore is an important part in anchor nodes location vis-à-vis the distance between anchors to the blind node. Integration of location capability into Wireless Sensor Network provides enablement in the location of network devices anywhere in the area of deployment, thereby making the network more valuable from the point of view of the application. Currently, there are several techniques which have been used to estimate ranges, most of the approaches which are dependent on a single frequency technique and those techniques are inaccurate in estimating the range, particularly in a multipath environment. The proposed work was to employ a dual-frequency phase difference of arrival technique for one-way propagation to capture ranges. Phase Difference of Arrival technique is a dual-frequency technique of ranging that offers better solution than already available single frequency ranging techniques. The technique has previously been used for radar application. Having evaluated the performance of this new technique for different frequency pairs with different frequency separation in different noise variance level, proof of the concept is provided using simulated data. The obtained results show that the proposed dual-frequency Phase-Difference of Arrival system is able to correctly find the location of, and track objects. Ranging simulation results show that frequency separation of 50MHz is best suited for one-way short-range application.

## ABSTRAK

Prinsip penglokasian adalah teknologi pengesanan yang membolehkan objek, orang dan asset dikesan. Ini pada asanya membolehkan objek dikesan untuk tujuan tindakan selanjutnya. Oleh yang demikian, teknik pengukuran jarak memainkan peranan penting dalam menganggarkan lokasi nod melalui pengukuran jarak di antara nod dan juga nod lain. Integrasi keupayaan penglokasian ke rangkaian pengesan wayarles membolehkan lokasi peranti rangkaian di mana-mana dalam penggunaan, membuat rangkaian lebih bermakna dari sudut aplikasi. Pada masa ini, terdapat beberapa teknik yang telah digunakan untuk menganggarkan jarak, kebanyakan teknik yang sedia ada bergantung kepada teknik frekuensi tunggal dan itu adalah kurang tepat dalam menganggarkan jarak, terutamanya dalam persekitaran pelbagai jarak. Projek yang dicadangkan adalah dengan menggunakan teknik perbezaan fasa ketibaan dua frekuensi bagi pergerakan isyarat sehala. Teknik perbezaan fasa ketibaan dua frekuensi adalah teknik peanggarkan jarak dwi-frekuensi yang menjanjikan penyelesaian yang lebih baik daripada teknik-teknik yang menggunakan frekuensi tunggal yang sedia ada. Teknik ini telah digunakan untuk aplikasi radar. Prestasi teknik ini dinilai dari segi pelbagai kombinasi frekuensi dan pelbagai kombinasi jarak pemisahan frekuensi di dalam keadaan pelbagai tahap gangguan isyarat dan ia dapat dibuktikan dengan menggunakan data simulasi. Hasil kajian menunjukkan bahawa cadangan teknik perbezaan fasa ketibaan dua frekuensi mampu untuk meanggarkan lokasi dan mengesan objek dengan betul. Hasil kajian menunjukkan bahawa jarak pemisahan frekuensi kurang daripada 50MHz adalah paling sesuai untuk aplikasi jarak dekat isyarat satu hala.

## TABLE OF CONTENTS

<b>CHAPTER</b>	<b>TITLE</b>	<b>PAGE</b>
	<b>DECLARATION</b>	ii
	<b>DEDICATION</b>	iii
	<b>ACKNOWLEDGEMENT</b>	iiv
	<b>ABSTRACT</b>	v
	<b>ABSTRAK</b>	vi
	<b>TABLE OF CONTENTS</b>	vii
	<b>LIST OF TABLES</b>	x
	<b>LIST OF FIGURES</b>	xi
	<b>LIST OF ABBREVIATIONS</b>	xiii
	<b>LIST OF APPENDICES</b>	xv
1	<b>INTRODUCTION</b>	<b>1</b>
	1.1 Introduction of the Research	1
	1.2 Statement of the Problem	3
	1.3 Objectives of the Study	4
	1.4 Scope of the Study	5
	1.5 Significance of the Study	5
	1.5.1 Why Range Estimation?	6
	1.5.2 Contribution of the Research to Knowledge	7

	1.6 Organization of the Thesis	7
2	<b>LITERATURE REVIEW</b>	<b>9</b>
	2.1 Overview	9
	2.2 Signal Propagation	10
	2.2.1 Free-space Model	11
	2.2.2 Two-ray Model	14
	2.2.3 Log-normal Shadowing Model	16
	2.3 Ranging Techniques	18
	2.3.1 Time of Arrival	18
	2.3.2 Time Difference of Arrival	20
	2.3.3 Angle of Arrival	21
	2.3.4 Received Signal Strength Indication	25
	2.3.5 Radio Interferometric Positioning System	28
	2.3.6 Swept Frequency technique	29
	2.4 The Proposed Technique	29
	2.4.1 The principle of operation of Radar	30
	2.4.2 Range estimation based on Dual-frequency signaling	32
3	<b>METHODOLOGY</b>	<b>37</b>
	3.1 Introduction	37
	3.2 Tools of Research	39
	3.2.1 Matlab	39
	3.2.2 Universal Software Radio Peripheral	40
	3.3 Possible obstacles to localization accuracy	44

4	<b>SIMULATION RESULTS AND ANALYSIS</b>	<b>45</b>
	4.1 Simulation Set-up	45
	4.2 Propagation models simulation results	48
	4.3 Range ambiguity	49
	4.4 Effect of Phase Noise	51
	4.5 Error Analysis	55
5	<b>CONCLUSION</b>	<b>57</b>
	5.1 Introduction	57
	5.2 Conclusion	57
	5.3 Recommendation for Future work	58
	<b>REFERENCES</b>	<b>61</b>
	Appendices	67

**LIST OF TABLES**

<b>TABLE NO.</b>	<b>TITLE</b>	<b>PAGE</b>
<b>4.1</b>	The operating frequencies used for Simulation	46
<b>4.2</b>	Distance error Vs Phase error	55

## LIST OF FIGURES

FIGURE NO.	TITLE	PAGE
1.1	Basic <i>Tx-Rx</i> signal transmission	3
2.1	Signal Propagation via Free Space Model	12
2.2	Signal Propagation via Two-Ray Model	14
2.3	Principle of Time of Arrival	18
2.4	Principle of location in Angle of Arrival Technique	22
2.5	Estimating range using Angle of Arrival	23
2.6	Trilateration approach of range estimation	26
2.7	Basic node formulation in Trilateration	27
2.8	Transmission of dual-frequency from a reader to an object	33
2.9	Phase difference Vs Range estimate	36
3.1	Flowchart describing the project schedule	39
3.2	Universal Software Radio Peripheral	42
3.3	Experimental set-up of USRP	40
4.1	Phase difference Vs. Distance relation	47
4.2	Dual frequency Estimator results	48
4.3	Propagation Models graphs	49
4.4	Range ambiguity analysis	51
4.5	Phase difference of two signals with time	52
4.6	Effect of phase noise on the signal propagation	53

<b>4.7</b>	Phase difference over 500 meters	55
<b>4.8</b>	Distance error Vs Phase error graph	56



**LIST OF ABBREVIATIONS**

AoA	-	Angle of Arrival
BFDM	-	Biorthogonal Frequency Division Multiplexing
BS	-	Base Station
CW	-	Carrier Wave
dB	-	Decibel
DDC	-	Digital Down Counter
DUC	-	Digital Up Counter
EM	-	Electromagnetic
$f$	-	Frequency
FFT	-	Fast Fourier Transform
FPGA	-	Field Programmable Gate Array
$G_E$	-	Emitter Gate
$G_R$	-	Receiver Gate
GHz	-	Gigahertz
I/O	-	Input/Output
Laser	-	Light Amplification by Stimulated Emission of Radiation
LOS	-	Line of Sight
LS	-	Least Squares
MATLAB	-	MATrix LABoratory
MHz	-	Megahertz
MIMO	-	Multiple-Input, Multiple-Output

MS	-	Mobile Station
OFDM	-	Orthogonal Frequency Division Multiplexing
OQAM	-	Offset Quadrature Amplitude Modulation
QAM	-	Quadrature Amplitude Modulation
RF	-	Radio Frequency
R <sub>x</sub>	-	Receiver
RFID	-	Radio Frequency Identification
RIPS	-	Radio Interferometric Positioning System
RSSI	-	Received Signal Strength Indication
RTLS	-	Real Time Locating System
SI	-	Spherical Interpolation
SNR	-	Signal-to-Noise Ratio
SOI	-	Signal of Interest
TDoA	-	Time Difference of Arrival
ToA	-	Time of Arrival
T <sub>x</sub>	-	Transmitter
USRP	-	Universal Software Radio Peripheral
WSN	-	Wireless Sensor Network

**LIST OF APPENDICES**

<b>APPENDIX</b>	<b>TITLE</b>	<b>PAGE</b>
A	Range versus Phase-difference code	65
B	Code for the effect of noise on signal propagation	66
C	Distance error versus Phase error code	69

## **CHAPTER 1**

### **INTRODUCTION**

#### **1.1 Introduction of the Research**

Ranges of unknown node with respect to several known nodes are required in locating the position of the unknown node. Currently, there are several techniques which have been used to estimate ranges, such as Time of Arrival (ToA), Time Difference of Arrival (TDoA), Angle of Arrival (AoA), Received Signal Strength Indication (RSSI) [1], Radio Interferometric Positioning System (RIPS), and others, described in the literature review. Most of the approaches are dependent on a single frequency technique and those techniques are inaccurate in estimating the range, particularly in a multipath environment.

Going by technological advances, it is observed that wireless networking technology has been experiencing a tremendous growth and widespread adoption in Communications Engineering. Integration of location capability into the Wireless Sensor Network (WSN) can aid the location of network devices anywhere in the area of deployment, making the network more valuable from the application point of view. A Wireless Sensor Network refers to a group of sensors, or nodes that are linked by a wireless medium to perform distributed sensing tasks. Connections between nodes are formed using such media as infrared devices or radios. Wireless sensor networks are usually used for such tasks as surveillance, widespread environmental sampling, security and health monitoring. They can be used in

virtually any environment, even those where wired connections are not possible, where the terrain is inhospitable, or where physical placement is difficult. Radiolocation is achieved by measuring one or more characteristics of the radio signal such as Received Signal Strength Indication, and Time-of-Arrival. Using these measurements, the ranges between devices in the network are estimated and the locations of the devices are computed based on the estimated nodes information [2].

The importance of localization which involves

(i) ranging,

(ii) positioning and

(iii) error optimization

has been applied in numerous modern applications such as personal and public security, healthcare and military [3]. This clearly shows the importance of Range estimation, to accurately find the location of the position of a blind or unknown node (i.e, a sensor node in an unknown position) such as an object, person, product, asset or vehicle.

Furthermore, crucial aspect of WSN operation produces low power consumption [2]. There is in recognition of the fact that multi-hop communication (messages are relayed by intermediate nodes) has the ability to improve energy efficiency by reducing the communication range required to convey information from a source to a destination [2]. While reducing range is attractive from power

consumption standpoint, the effect of communication range on range estimation and location estimation accuracy is still being exploited [2].

There has been the usage of distance estimation using phase measurement in many areas of Science and Engineering [3]. Particularly in this work, two signals with different frequencies will be transmitted from the transmitter to a receiver. The signals will arrive at the receiver at different phases. The corresponding phase difference from these two transmitted signals will be processed to evaluate the distance between the transmitting and receiving nodes [3]. This concept is illustrated in Figure 1.1.

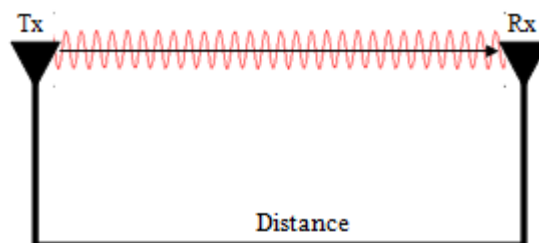


**Figure 1.1** Basic *Tx-Rx* signal transmission

## 1.2 Statement of the Problem

Due to the inaccuracy which the single frequency technique poses especially when transmitted signals are highly faded at some frequencies, it has become necessary to employ dual frequencies to estimate the required range. This involves transmitting signals using two different frequencies to an unknown node. This is necessary because if one signal is transmitted, there is every tendency that it will fade at some point along the line. This will certainly affect the outcome of the range

estimate carried out with it. By employing dual-frequency, obviously, the two signals would not fade out at the same time. Even one fades, the other will be available to complete the task. The signals, thereby, arrive at the node at different phases. The difference in the phases of the arriving signals would then be used to adequately locate and estimate the node. Therefore, the problem statement for this research is stated as follows: “How to provide frequency diversity for robust range estimation in a wireless communication environment”.

### **1.3 Objectives of the Study**

The task of performing this project work necessitated some objectives to be realized. The following are therefore the objectives set out for this research work:

- (i) To study the signal propagation in short-range communication,
- (ii) To simulate range estimation using Phase Difference of Arrival (PDoA) technique,
- (iii) To analyze the range estimation through range ambiguity, effect of noise, and error analysis.

## 1.4 Scope of the Study

The scope of this work is; Investigating range estimation using dual-frequency technique, in order to find an acceptable and best-suited frequency separation for a short-range one-way propagation scenario.

## 1.5 Significance of the Study

Location estimation from range measurements can be viewed as an error minimization approach, for which Least squares (LS) is a classic approach. However, there are aspects of the problem which, when hypothesized, could allow better results than the LS method with the same multipath ToA datasets. First, the ToA error (hence range error) due to multipath can only be positive. A negative range error would imply superluminal propagation. Therefore, in any physically consistent set of range measurements, it is impossible for the true location to lie outside of any of the circles of measured range radii about the respective base-stations. It is easily demonstrated that LS solutions are not consistent with this physical principle.

Secondly, by studying the location estimates of a human presented with a graphical representation of the base-station map and overlaid circles from sets of ranging estimates (to known), it could be found that the best estimates tend to be based on a visually apparent subset of range circles which tend to the most self-consistent in terms of nearly describing a point intersection. This is rather different to LS in which the most outlying range circles actually have more than a proportional influence on the solution. One could weight each range measurement in an LS



formulation, but this would require ancillary means to assign reliability estimates to each range measurement. In view of the above therefore;

- (1) Range-based localization of object is able to provide adequate precision as it exploits measurements of physical quantities related to signals travelling between the anchor and the object [4].
- (2) Through range-estimation over dual-frequency pairs, the effect of noise can be greatly reduced in the communication environment.
- (3) By using range-based approach therefore, error minimization is adequately guaranteed [5].

Hence, we can look at this sub-topic under the following sub-divisions:

### **1.5.1 Why Range Estimation?**

In wireless communication technology, there is a rapid development of the need for identification, location and tracking of objects such as products, assets, and personnel, electronically. It has become one of the primary means to construct a Real-Time Locating System (RTLS) that tracks and identifies the location of objects in real time.

Interestingly, there exists a relationship between range-estimates and:

- (1) Bandwidth, whereby precision increases with bandwidth, but carries diminishing returns with the additional expense;
- (2) center frequency, whereby lower frequencies penetrate materials better (where there is a building between the transmitter and the receiver).

The technique employed in this work, has the potential of estimating the position of an unknown node accurately, provided that the distances between two or more known nodes to the unknown node are well known. Hence, to have high accuracy in positioning, the need of a robust ranging technique is required [3].

### **1.5.2 Contribution of the Research to Knowledge**

With the single-frequency technique, when the transmitted signal is severely faded, the technique will likely produce phase that is unreliable, and subsequently, yield unreliable range estimation from the received signal. The employed dual-frequency technique has the capability of taking care of this problem. Also, noise has a greater effect on single-frequency signal, which the dual-frequency technique is able to minimize to the barest level.

## **1.6 Organization of the Thesis**

The field of Signal Processing has grown enormously in the past few decades to encompass and provide firm theoretical background for a large number of individual areas. Since range estimation, for the most part, relies on the theory of Signal processing, it is shown as a major unifying influence for the entire work.

Chapter 1 introduces the general concept of the research work, providing the statement of the problem, the objectives and the significance of the study.

Chapter 2 extensively discusses the literature review, reviewing the previous work done in recent times on the topic and then, reviewing the related topics.

Chapter 3 dwells on the methodology of the research, including the tools employed in carrying out the research.

Chapter 4 presents the simulation results and the analysis.

Chapter 5 is the conclusion of this report.

## CHAPTER 2

### LITERATURE REVIEW

#### 2.1 Overview

Ranging is a phenomenon used widely for the purpose of identifying and localizing objects electronically. It is able to offer substantial advantages for businesses, thereby allowing automatic inventory and tracking on the supply chain. This new technology plays a key role in pervasive networks and services. Indeed, data can be stored and remotely retrieved through ranging, thereby enabling real-time identification of devices and users. The functionality of ranging technology also finds application the area of indoor navigation, precise real-time inventory, and in library management to retrieve persons or objects, control access, and monitor events [6].

For Range-free techniques, the actual distance measurements are not required since the connectivity or any information available such as hop-count can be used as estimate distance for positioning estimation. The examples of Range-free techniques are proximity-based localization, one-hop localization and multi-hop localization [3].

However, Range-based localization approach get more attention in research field since positioning is more accurate when compared to Range-free approach [3].

Range estimation, which uses single frequency, suffers from large range uncertainty and ambiguity [7]. This is because such estimation based on a single frequency  $f$ , has infinite range estimate solution, separated just by only half of the corresponding wavelength [7]. This is explained well in section 2.3.1. Drastic reduction in range ambiguity can be achieved in two ways. One is by lowering the transmitted signal frequency so as to increase the distance between two possible consecutive range estimates, thereby ruling out those range estimates inconsistent with the nature of the scene [7]. Secondly, the reduction in range ambiguity is also possible through increase in distance, making it larger than the difference between the lower and the upper bounds on target location [7]. However, the range ambiguity can be totally eliminated by employing dual-frequency pairs in the transmission of signals from the transmitter to the receiver [8].

## **2.2 Signal Propagation**

Basically, there are two ways of transmitting an electro-magnetic (EM) signal, namely either through a guided medium or through an unguided medium. Guided mediums such as coaxial cables and fiber-optic cables are far less hostile toward the information carrying EM signal than the wireless or the unguided medium. It presents challenges and conditions which are unique for this kind of transmissions [9]. As a signal travels through the wireless channel, it undergoes many kinds of propagation effects such as reflection, diffraction and scattering. This, of course is due to the presence of buildings, mountains and other such obstructions.

Reflection occurs when the EM waves impinge on objects which are much greater than the wavelength of the traveling wave. Diffraction is a phenomena occurring when the wave interacts with a surface having sharp irregularities. Scattering occurs when the medium through the wave is traveling contains objects which are much smaller than the wavelength of the EM wave.

These varied phenomena's lead to large scale and small scale propagation losses. Due to the inherent randomness associated with such channels they are best described with the help of statistical models. Models which predict the mean signal strength for arbitrary transmitter receiver distances are termed as large scale propagation models. These are termed so because they predict the average signal strength for large  $Tx-Rx$  separations, typically for hundreds of kilometers.

Further analysis was carried out with the signal propagation via the following models:

### **2.2.1 Free-space Model**

Generally, EM signals when traveling through wireless channels, usually experience fading effects due to various effects, but in some cases the transmission is with a direct line of sight such as is obtained in satellite communication. Free space model, depicted in Figure 2.1 predicts that the received power decays as negative square root of the distance.

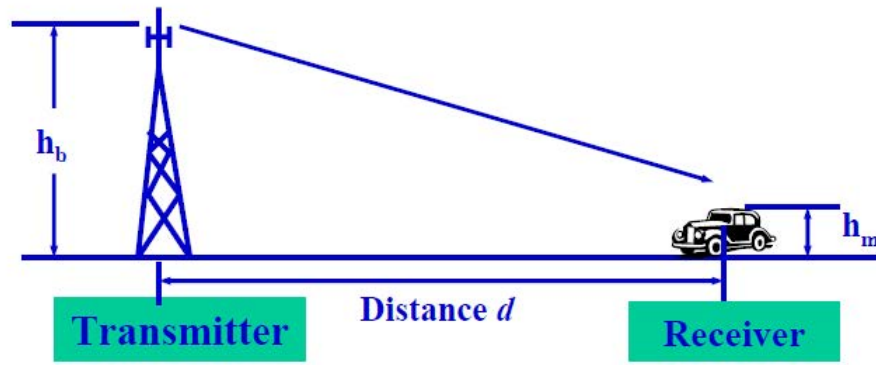


**Figure 2.1** Signal propagation via Free-space model

Friis free space equation is given by,

$$P_r(d) = \frac{P_t G_t G_r \lambda^2}{(4\pi)^2 d^2 L} \quad (2.1)$$

where  $P_t$  is the transmitted power,

$P_r(d)$  is the received power,

$G_t$  is the transmitter antenna gain,

$G_r$  is the receiver antenna gain,

$\lambda$  is a factor which depends on the propagation environment,

$d$  is the  $Tx-Rx$  separation and

$L$  is the system loss factor which depends upon line attenuation, filter losses and antenna losses and not related to propagation.

The gain of the antenna is related to the effective aperture of the antenna which in turn is dependent upon the physical size of the antenna given as follows:

$$G = \frac{4\pi A_e}{\lambda^2} \quad (2.2)$$

where  $A_e$  = effective aperture of the antenna.

The path loss, which represents the attenuation suffered by the signal as it travels through the wireless channel is given by the difference of the transmitted and received power in dB and is expressed as:

$$PL(dB) = 10 \log \left( \frac{P_t}{P_r} \right) \quad (2.3)$$

The fields of an antenna can be classified in two broad regions, namely the far field and the near field. It is in the far field that the propagating waves act as plane waves and the power decays inversely with distance. The far field region is also termed as Fraunhofer region and the Friis equation holds in this region. Hence, the Friis equation is used only beyond the far field distance,  $d_f$ , which is dependent upon the largest dimension of the antenna as:

$$d_f = \frac{2D^2}{\lambda} \quad (2.4)$$

where  $d_f$  = far-field distance, and

$D$  is the largest dimension of the antenna.

Also we can see that the Friis equation is not defined for  $d = 0$ . For this reason, we use a close in distance,  $d_0$ , as a reference point. The power received,  $P_r(d)$ , is then given by:

$$P_r(d) = P_r(d_0) \left( \frac{d_0}{d} \right)^2 \quad (2.5)$$



The major drawback in this technique is that the RSSI-based systems usually need on-site adaptation in order to reduce the severe effects of multipath fading and shadowing in indoor environments [10].

### 2.2.2 Two-ray Model

Two-ray model is also known as Ground Reflection model. It is a simple model for propagation over ground, pictorially represented as shown in Figure 2.2.

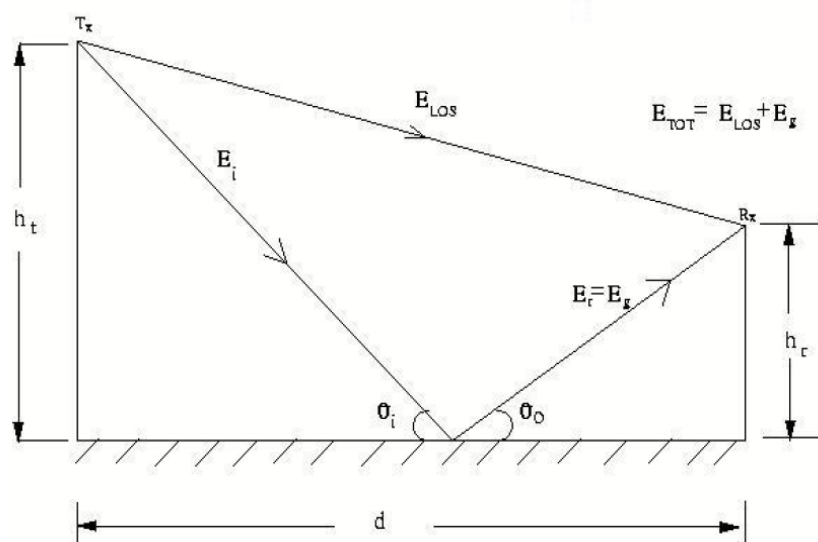


**Figure 2.2** Signal propagation via Two-ray model

Here, two components of transmitted signals arrive at the receiver – one LOS and the other reflected from the ground. For small angle of incidence, it is assumed that the reflection coefficient,  $\Gamma = -1$ .

At large distances compared to the antenna heights the two components will have approximately equal amplitude and a small phase difference given by:

$$\theta_\delta = \frac{2\pi\delta}{\lambda} \quad (2.6)$$

where  $\delta \approx \frac{2h_t h_r}{d}$ .

For large  $d$  ( $\gg \sqrt{h_t h_r}$ ), it can be shown that the received power is,

$$P_r = P_t G_t G_r \frac{h_t^2 h_r^2}{d^4} \quad (2.7)$$

where  $P_t$  = transmitted power,

$G_t$  = gain of the transmitter,

$G_r$  = gain of the receiver,

$h_t$  = height of the transmitter above ground level,

$h_r$  = height of the receiver above ground level, and

$d$  = distance between the transmitter and the receiver.

For this model, the path loss varies as  $d^4$ , the square of the antenna height and is independent of the frequency [2].

### 2.2.3 Log-normal Shadowing Model

In radio communications, the levels of the received signal usually decrease as the distance between the transmitter and the receiver increases. This phenomenon is known as path-loss. Attenuation of radio signals due to the path-loss effect has been modeled by averaging the measured signal powers over long times and over many distances around the transmitter. The averaged power at any given distance to the transmitter is referred to as the area mean power  $P_a$  (in Watts or milli-Watts). The path-loss model states that  $P_a$  is a decreasing function of distance  $r$  between transmitter and the receiver and can be represented by a power law:

$$P_a(r) = c \left( \frac{r}{r_0} \right)^{-\eta} \quad (2.8)$$

where  $P_a$  = power received at the receiver,

$c$  = velocity of electromagnetic wave,

$r$  = distance between transmitter and receiver, and

$r_0$  = reference distance.

In Equation (2.8),  $r_0$  is a reference distance. Parameter  $\eta$  is the path-loss exponent which depends on the environment and terrain structure and can vary between 2 in free space to 6 in heavily built urban areas. The constant  $c$  depends on the transmitted power, the receiver and the transmitter antenna gains and the wavelength. The path-loss model is often used in the study of wireless ad-hoc networks. However, this model could be inaccurate because in reality, the received power levels may show significant variations around the area mean power. This model is the log-normal shadowing model, and allows for random power variations around the area mean power. Let the received power at distance  $r$  from the transmitter be denoted by  $P(r)$ . In the log-normal shadowing model the basic assumption is that the logarithm of  $P(r)$  is normally distributed around the logarithmic value of the area mean power [11]:

$$10\log_{10}(P(r)) = 10\log_{10}(P_a(r)) + x \quad (2.9)$$

In Equation (2.9),  $x$  is a zero-mean normal distributed random variable (in dB) with standard deviation  $\sigma$  (also in dB). The standard deviation is larger than zero and, in some special cases where there are severe signal fluctuations due to irregularities in the surroundings of the receiving and transmitting antennas, it can be as high as 12 [12]. It could be noticed that if  $\sigma$  is assumed to be equal to zero, the log-normal model will be the same as the path-loss model. So, the path-loss model can be seen as a specific case of the more general log-normal model.

## 2.3 Ranging Techniques

Work has been carried out in the area of estimating ranges of some objects using various techniques. While many techniques employ single-frequency, few other techniques employ dual-frequency. Some of these techniques are hereby discussed, in terms of their modes of operation. Their drawbacks and shortcomings are clearly stated.

### 2.3.1 Time of Arrival

In the Time of Arrival (ToA) technique, the one-way propagation time of the signal traveling between a mobile station (MS) and each of the base stations (BSs) is measured, and this provides a circle centered at the BS on which the MS must lie. The ToA measurements are then converted into a set of circular equations, from which the MS position can be determined with the knowledge of the BS geometry. Figure 2.3 shows the diagrammatic representation of the principle behind ToA.

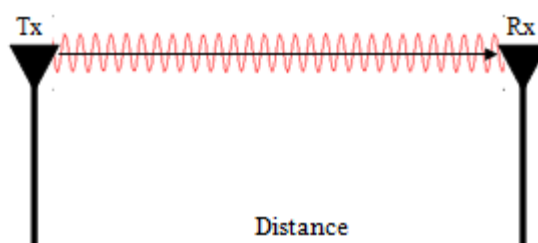


**Figure 2.3** Principle of Time of Arrival

Basically, what is needed here is to estimate the range (distance) between the Transmitter ( $T_x$ ) and the Receiver ( $R_x$ ). And this is done by sending the signal from the transmitter and then taking note of the time it takes the signal to arrive at the receiver. Then, the required estimation is carried out using:

$$R(t) = c \times t \quad (2.10)$$

where  $R(t)$  is the required range,

$c$  is the velocity of electromagnetic wave, and

$t$  is the time of travel for the signal.

A straightforward approach for determining the MS position is to solve the nonlinear equations relating these measurements directly, but it is computationally intensive [13]. Apart from the direct methodology, another common technique that avoids solving the nonlinear equations is to linearize them, and then, the solution is found iteratively. However, this latter approach requires an initial estimate and cannot guarantee convergence to the correct solution unless the initial guess is close to it.

To allow real-time implementation and ensure global optimization, the idea of the spherical interpolation (SI) in Time Difference of Arrival (TDoA)-based location is adopted. Here, the nonlinear hyperbolic equations are reorganized into a set of linear equations by introducing an intermediate variable, which is a function of the source position. However, the SI estimator solves the linear equations directly

via least squares (LS) without using the known relation between the intermediate variable and the position coordinate.

In ToA technique of estimating range, the distance between a reference point and the target is proportional to the propagation time of signal. ToA-based systems need at least three different measuring units to perform adequate positioning in 2-D. This is a major drawback of this technique. Moreover, the technique also requires that all transmitters and receivers are precisely synchronized so that the receiver can know when the transmitter starts sending the signal.

### **2.3.2 Time Difference of Arrival**

With the Time Difference of Arrival (TDoA) technique, two observing antennas are held a fixed distance from each other. These distances are typically large. Receivers with pre-detection outputs are then attached to the two antennas, and the two resultant outputs are cross-correlated. The peak output from the cross-correlation is a measure of the TDoA between the observation points. A line of position may be calculated from the cross-correlation peak. In the case of a wide-band signal of interest (SOI) in an environment of narrow-band interference, the determination of the cross-correlation peak is extremely difficult and often impossible due to equipment limitations. This is particularly true if the interference is of smaller bandwidth than the SOI. Such interference then has a broad cross-correlation function which typically obscures the correlation function of the SOI [14].

TDoA is very much related to ToA in the sense that both employ single frequency. The only difference is that in TDoA, the single frequency are sent out from the transmitter two times, taking proper note of the time that the signals were sent. This is necessary in order to use the difference in time of the arrivals of the signals for the purpose of estimating the required range. The principle of TDoA lies on the principle of determining the relative location of a targeted transmitter by employing the difference in time at which the signal emitted by a target arrives at multiple measuring units. It is such that three fixed receivers give two TDoAs and thus provide an intersection point that is the estimated location of the target. The major drawback with this technique is that it requires a precise time reference between the measuring units especially in indoor environments where a Line-of-Sight (LOS) is rarely available [9].

### 2.3.3 Angle of Arrival

By Angle of Arrival (AoA) is meant the angle between the propagation direction of an incident wave and some reference direction, which is known as orientation [13]. Orientation, defined as a fixed direction against which the AoAs are measured, is represented in degrees in a clockwise direction from the North. When the orientation is  $0^0$  or pointing to the North, the AoA will be absolute, otherwise, it will be relative. One common approach to obtain AoA measurements is to use an antenna array on each sensor node.

AoA technique consists in calculating the intersection of several direction lines, each originating from a beacon station or from the target [15]. As shown in Figure 2.4, the Triangulation approach, which the AoA technique is premised upon,



involves measuring the angle of arrival of at least two reference points. The estimated position of the target corresponds to the intersection of the lines defined by the angles.

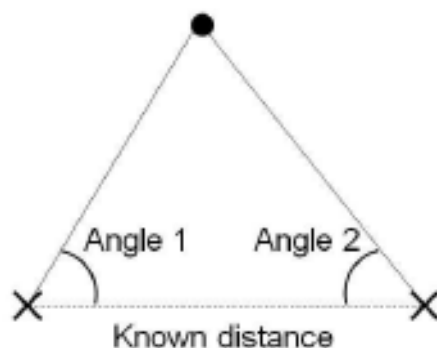


**Figure 2.4** Principle of location in Angle of Arrival technique

A common occurrence in a typical urban sensing environment is multipath. It could be noted that the effect of multipath is very similar to the presence of a target. With a propagation environment with two or more paths, the phase of the received signal corresponds to neither the target (direct path), nor that of the indirect path [16].

In order to use the principle of AoA to estimate a required range, consider Figure 2.5.

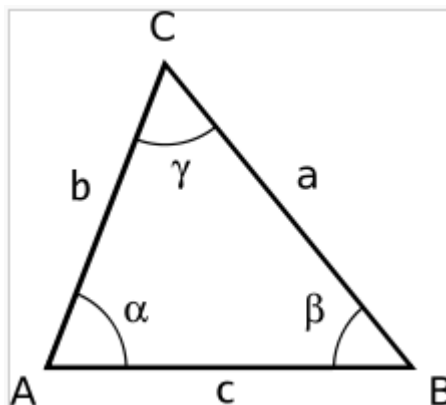


**Figure 2.5** Estimating range using Angle of Arrival technique

A general form of triangle has six (6) main characteristics as shown in Figure 2.5, having

- (i) three linear lengths  $a$ ,  $b$  and  $c$ , and
- (ii) three angles  $\alpha$ ,  $\beta$  and  $\gamma$ .

Now, in this case of AoA, the length  $c$  is known, as well as angles  $\alpha$  and  $\beta$ . From the triangle, the third angle can be calculated from:

$$\gamma = 180^{\circ} - (\alpha + \beta) \quad (2.11)$$

since the sum of all the three angles give  $180^{\circ}$ . The law of sines is now used which mathematically states that:

$$\frac{a}{\sin \alpha} = \frac{b}{\sin \beta} = \frac{c}{\sin \gamma} \quad (2.12)$$

from where the range is calculated as:

$$b = \frac{c \sin \beta}{\sin \gamma} \quad (2.13)$$

and

$$a = \frac{c \sin \alpha}{\sin \gamma} \quad (2.14)$$

The effect of multipath differs depending on the location of the target. Because the phase of the combined signal is highly nonlinear with respect to the multipath strength, the phase of the combined signal is close to that of the target return signal if the multipath signal is weak compared to direct path return. Otherwise, the phase will be highly distorted and thus cannot render meaningful range information [16].

The major drawback with this technique is that a directional antenna is required at the transmitter. The mechanism needed to rotate the directional antenna involves expensive equipments and hence complex.

### 2.3.4 Received Signal Strength Indication

Due to the wireless networking boom and demand for wireless networking infrastructure which is high, several products that enable wireless networking, Bluetooth, and other technologies are very much available and can be fitted to almost any mobile device available today. Furthermore, it can be expected that WSN play a significant role in the future of ubiquitous computing. As a result, Received Signal Strength Indication (RSSI) technique came into existence, to derive location estimates of wireless signals. RSSI based localization techniques generally has two phases – a training phase and an estimation phase [17]. In the training phase, a mapping between wireless signal strength and various predefined positions in the environment is established. This is typically achieved by collecting RSSI samples at the predefined locations. In most cases, the environment is divided into cells in order to define these locations. In the estimation phase, an estimate of the target's location is computed using the signal strength mapping (otherwise known as wireless map) via probabilistic or deterministic techniques.

Thus, RSSI based location estimation techniques are divided into two broad techniques, namely deterministic technique and probabilistic technique. For the use of a deterministic technique, the physical area making up the environment is first divided into cells [1]. Next, the training is performed in which readings are taken from several fixed, known access points. Finally, localization is performed by executing a determination phase in which the most likely cell is selected by determining which cell the new measurement fits best. Probabilistic methods, on the other hand, construct a probability distribution over the target's location for the physical area making up the environment. In order to estimate the location of the target, different statistics like the mode of the distribution or the area with highest probability density may be used. While probabilistic techniques provide more precision, a trade-off between computational overhead and precision is introduced.

RSSI technique therefore, is premised on the principle that the attenuation of emitted signal strength is a function of the distance between the emitter and the receiver. The target, in this technique, can thus be localized with at least three reference points and the corresponding signal path losses due to propagation [2]. The approach, called Trilateration approach, is illustrated in Figure 2.6, whereby, the position of the target is estimated by evaluating its distances from three reference points [14, 18].

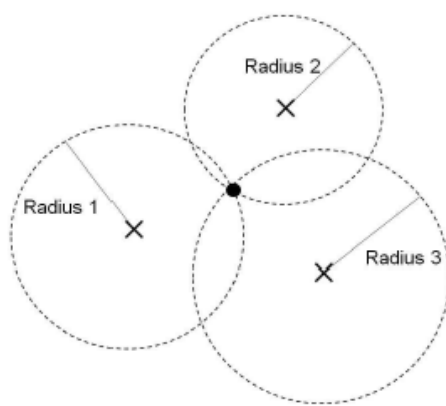


**Figure 2.6** Trilateration approach of range estimation

The concept of Trilateration is illustrated in Figure 2.7.

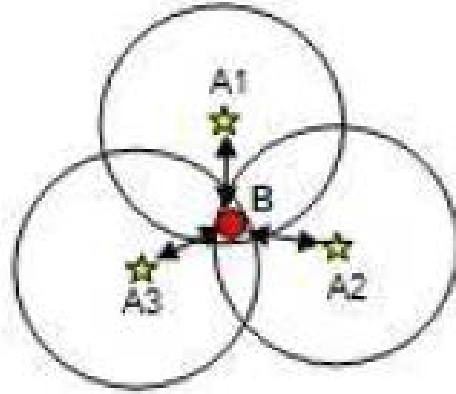


**Figure 2.7** Basic node formulation in Trilateration

Referring to Figure 2.7, assuming that  $A_1$ ,  $A_2$  and  $A_3$  are the anchor nodes in known locations while  $B$  is a blind node in an unknown location. Let coordinates of  $A_1$ ,  $A_2$  and  $A_3$  be  $(x_1, y_1)$ ,  $(x_2, y_2)$  and  $(x_3, y_3)$  respectively while coordinate of  $B$  is  $(x, y)$ . Now, let us assume that distances between  $A_1$ ,  $A_2$  and  $A_3$  toward  $B$  are  $d_1$ ,  $d_2$  and  $d_3$  respectively. So, through Trilateration, coordinate  $x$  and  $y$  can be calculated as [3]:

$$x = \frac{v_a - y_1(y_3 - y_2)}{(x_3 - x_2)} \quad (2.15)$$

and

$$y = \frac{v_b(x_3 - x_2) - v_a(x_1 - x_2)}{(y_1 - y_2)(x_3 - x_2) - (y_3 - y_2)(x_1 - x_2)} \quad (2.16)$$

where,

$$v_a = \frac{(d_2^2 - d_3^2) - (x_2^2 - x_3^2) - (y_2^2 - y_3^2)}{2} \quad (2.17)$$

and

$$v_b = \frac{(d_2^2 - d_1^2) - (x_2^2 - x_1^2) - (y_2^2 - y_1^2)}{2} \quad [19] \quad (2.18)$$

Several models have been proposed empirically and theoretically, in order to translate the difference between the transmitted and the received signal strength into distance estimation. The signal propagation theory behind RSSI can further be understudied through the following topic, having further sub-topics:

### **2.3.5 Radio Interferometric Positioning System**

The Radio Interferometric Positioning System (RIPS) is similar to the proposed technique in that it employs dual-frequency for its operation [20].

The principle of optical interference is presently used in interferometers for metrology, for high precision distance measurements over short distances and for the definition of the meter. The development of interferometers dates back to 1880, when A. A. Michelson had his first interferometer built in Germany [21]. A first measurement of the meter in terms of light waves followed in 1889. For his work on interferometers, Michelson received the Nobel Prize in Physics in 1907.

The basic principle of an interferometer is that two sinusoidal signals are transmitted with slightly different frequencies. A reflecting tag (object) at the unknown node reflects the signals back to the transmitter. The difference in the frequencies of the arrived signals at the transmitter is then used to estimate the location of the object.

The major drawback with this technique is that four (4) nodes are needed for its successful operation. If one node fails, then the range becomes difficult to estimate.

### **2.3.6 Swept Frequency technique**

Other techniques such as Swept Frequency technique and Pulse Compression technique have also been employed [7], to increase the unambiguous range though, but the operational logistics and system requirements related to cost, hardware, and real-time processing, make the realization of such techniques more tasking for urban sensing applications [7].

Generally, the proposed dual-frequency technique however, will meet the necessary requirements and is likely to emerge as one of the leading technologies in a multipath environment [7].

## **2.4 The Proposed Technique**

The proposed technique for this project work is similar to the principle of operation of Radar (an acronym for Radio Detection And Ranging). The similarity of both Radar and the proposed technique for this project work is that they both employ dual-frequency to estimate ranges of objects. However, Radar operates using



2-way propagation scenario while the proposed technique for this project will operate on one-way propagation scenario.

#### 2.4.1 The principle of operation of Radar

Radar is an object detection system that uses radio waves to determine the range, angle or velocity of objects. A Radar transmits radio waves that reflects from any object in its path. The received waves are then processed to determine the above named properties of the object.

The power returning to the receiving antenna is given by:

$$P_r = \frac{P_t G_t A_r \sigma F^4}{(4\pi)^2 R_t^2 R_r^2} \quad (2.19)$$

where  $P_t$  = transmitted power,

$G_t$  = gain of transmitting antenna,

$\sigma$  = Radar cross-section,

$F$  = pattern propagation factor,

$R_t$  = distance from the transmitter to target,

$R_r$  = distance from the target to the receiver,

$A_r$  = effective aperture (area) of receiving antenna given by:

$$A_r = \frac{G_r \lambda^2}{4\pi} \quad (2.20)$$

where  $\lambda$  = transmitted wavelength, and

$G_r$  = gain of receiving antenna.

However, in common case where transmitter and receiver are at the same location, then

$$R_t = R_r \quad (2.21)$$

which implies that:

$$P_r = \frac{P_t G_t A_r \sigma F^4}{(4\pi)^2 R^4} \quad (2.22)$$

### 2.4.2 Range estimation based on Dual-frequency signaling

Consider that a dual-frequency signal is transmitted from a transmitter using frequencies  $f_1$  and  $f_2$  to an object [22], located at an unknown point, as shown in Figure 2.8. The transmitted signals at frequency  $f_i$ ,  $i = 1, 2$ , can be expressed as [16],

$$s_i(t) = \rho e^{-j\phi_i(t) + n_0(t)}, \quad i = 1, 2, \quad (2.23)$$

where  $s_i(t)$  is the dual-frequency waveforms from the transmitter,

$\rho$  is the range-dependent amplitude,

$\phi_i(t)$  is phase of the signal corresponding to the  $i$ -th frequency of operation,

and

$n_0(t)$  is the Gaussian noise introduced into the signals [22].

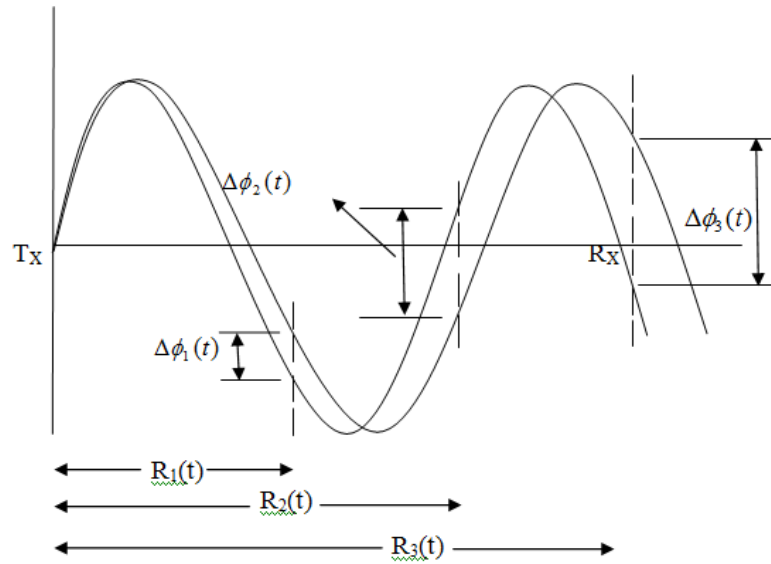


**Figure 2.8** Transmission of dual-frequency from a reader to an object

Now,

$$\phi_i(t) = 2\pi(f_i t + x) \quad (2.24)$$

Measuring both phases in the  $[0, 2\pi]$  range, then we have

$$\phi_1(t) = 2\pi f_1 t + 2\pi n \quad (2.25)$$

and

$$\phi_2(t) = 2\pi f_2 t + 2\pi n \quad (2.26)$$

Now, the velocity of electromagnetic wave propagation is related to both the time of arrival of the signal from the transmitter to the receiver [23], and also the distance between the transmitter and the receiver as follows:

$$c = \frac{R(t)}{t}, \quad (2.27)$$

where  $c$  = the velocity of electromagnetic wave propagation,

$R(t)$  = the desired range, and

$t$  = time of arrival of the signal from the transmitter to the receiver.

From equation (2.27),

$$t = \frac{R(t)}{c} \quad (2.28)$$

Substituting Equation (2.28) into Equations (2.25) and (2.26) gives,

$$\phi_1(t) = \frac{2\pi f_1 R(t)}{c} + 2\pi m, \quad (2.29)$$

and

$$\phi_2(t) = \frac{2\pi f_2 R(t)}{c} + 2\pi n \quad (2.30)$$

where  $m$  and  $n$  are unknown integers.

Now, the phase difference at the receiver, from Equations (2.29) and (2.30) is given by:

$$\Delta\phi(t) = \phi_2(t) - \phi_1(t) \quad (2.31)$$

$$\begin{aligned} &= \frac{2\pi f_2 R(t)}{c} + 2\pi n - \frac{2\pi f_1 R(t)}{c} - 2\pi m \\ &= \frac{2\pi R(t)}{c} (f_2 - f_1) - 2\pi(m - n) \end{aligned} \quad (2.32)$$

Making  $R(t)$  the subject of the expression in Equation (2.17) gives,

$$R(t) = \frac{c\Delta\phi(t)}{2\pi(f_2 - f_1)} - \frac{c(m - n)}{(f_2 - f_1)} \quad (2.33)$$

The second term in Equation (2.33) induces ambiguity in range, which means that for the same phase difference, the range estimate can assume infinite values [16] separated by the maximum unambiguous range  $R_{max}$  [22]. An example of the phase difference versus the range estimate is shown in Figure 2.7, where the frequency separation is  $\Delta f = 26 \text{ MHz}$  and the actual range is  $R = 7.6 \text{ m}$  [22]. So, to remove this ambiguity, we assume that  $m = n$ . Hence, Equation (2.33) reduces to,

$$R(t) = \frac{c\Delta\phi(t)}{2\pi\Delta f} \quad [7] \quad (2.34)$$

where  $\Delta f = f_2 - f_1$  [13, 21].

However, the maximum unambiguous range is given by [24]:

$$\begin{aligned} R_{\max} &= \frac{c}{2\Delta f} & (2.35) \\ &= \frac{3 \times 10^8}{2 \times 26 \times 10^6} \\ &= 5.77 \text{ m} \end{aligned}$$

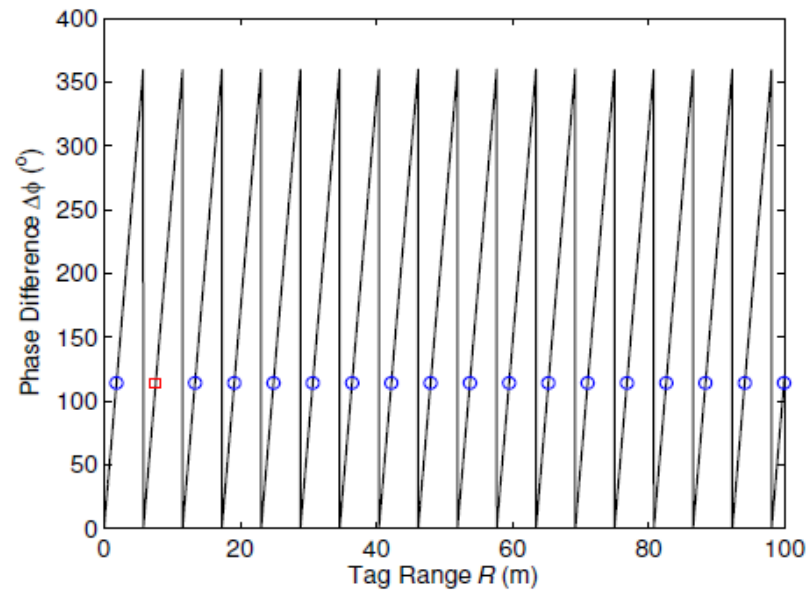


**Figure 2.9** Phase difference versus Range estimate

For clarity, the actual range ( $R$ ) at 7.6 m is marked by a square and the estimated ranges at repetitive positions 1.83 m, 13.37 m, 19.14 m, . . . , separated by  $R_{max} = 5.77$  m are marked by circles [22].

## CHAPTER 3

### METHODOLOGY

#### 3.1 Introduction

The methodology involves a body of methods, rules, and postulates employed in carrying out this work. It captures the analysis of the principles or procedures of inquiry into the field of ranging estimation.

This project work is carried out following the schedule outlined below:

- (1) Critical understudying the signal propagation processes and techniques.
- (2) a) Reviewing the previous work done, including the techniques which have been developed.  
  
b) Understudying through research, the approach of the employed dual-frequency technique.
- (3) Carrying out simulations of PDoA in the Matlab environment.
- (4) Studying and analyzing the phase characteristics of the received signal.



- (5) Analyzing the Range ambiguity, effect of noise and error on the range estimation.
- (6) Drawing out the findings.

Figure 3.1 captures the above schedule in flowchart form.

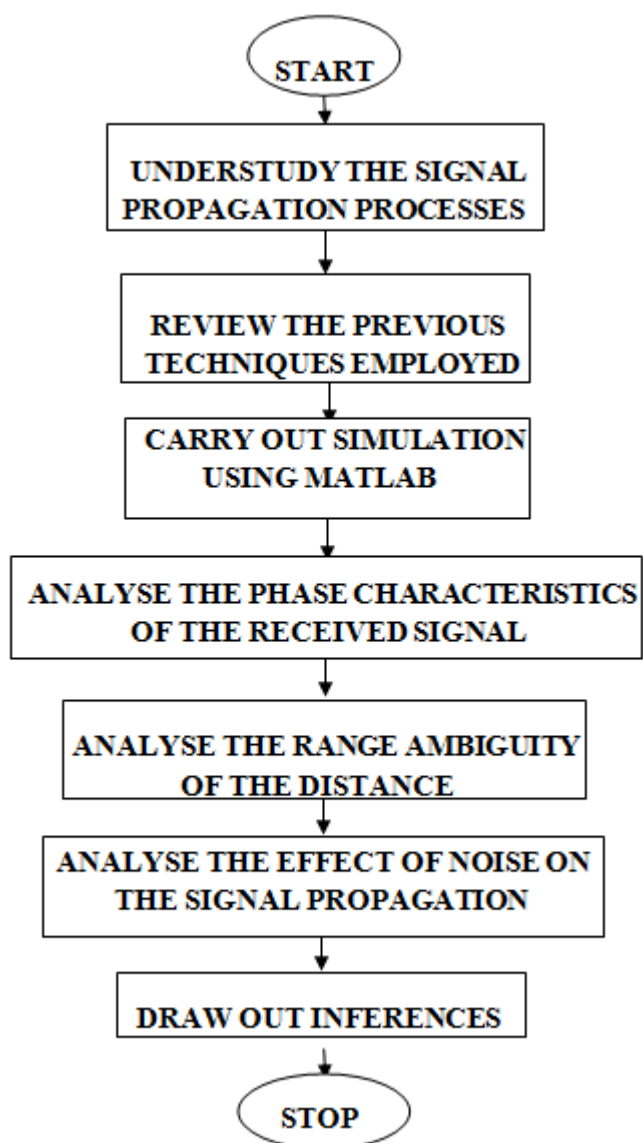


**Figure 3.1** Flowchart describing the project schedule

## **3.2 Tools of Research**

The employable tools available for carrying out this research work are basically:

- (1) Matlab, for simulation, and
- (2) Universal Software Radio Peripheral.

### **3.2.1 Matlab**

MATLAB (which stands for MATrix LABoratory) is a high-level technical computing language and interactive environment for algorithm development, data visualization, data analysis, and numerical computation. It is a special-purpose computer program optimized to perform Engineering and scientific calculations. Using Matlab, technical computing problems can be solved faster, especially when interfaced with programs written in programming languages such as C, C++, Java, Python and Fortran.

Matlab is more than a fancy calculator. It is an extremely useful and versatile tool in Communication Engineering simulation. Even if a little is known about Matlab, one can use it to accomplish wonderful things. The hard part, however, is figuring out which of the hundreds of commands, scores of help pages, and thousands of items of documentation one needs to look at to start using it quickly and efficiently.

Many signal processing researchers now use the Matlab technical computing language to develop their algorithms because of its ease to use, powerful library functions and convenient visualization tools.

The aim here is not to go into the details of the operations of Matlab, but to mention it as a tool employed for simulation in this project work. The codes for the simulations of this work are presented in the Appendices.

### **3.2.2 Universal Software Radio Peripheral**

The Universal Software Radio Peripheral (USRP) is a transceiver device which enables engineers to rapidly design and implement powerful and flexible software radio systems [25]. Figure 3.2 shows the board diagram of a USRP. The intuitive USRP design, coupled with a broad selection of daughter-boards covering a wide range of frequencies, helps in getting the needed software radio up and running quickly.



**Figure 3.2** Universal Software Radio Peripheral

What is simply needed is to download GNU Radio, a complete open source software radio and signal processing package, and the USRP is ready to use. Once the software is installed and the USRP is plugged into a host computer, it is ready to transmit and receive a virtually limitless variety of signals. The USRP can simultaneously receive and transmit on two antennas in real time. All sampling clocks and local oscillators are fully coherent, thus allowing the creation of MIMO (Multiple-Input, Multiple-Output) systems [26].

In the USRP, high sample-rate processing takes place in the Field Programmable Gate Array (FPGA), while lower sample-rate processing happens in the host computer. The two onboard Digital Down-Converters (DDCs) mix, filter, and decimate (from 64 MS/s) incoming signals in the FPGA. Two Digital Up-Converters (DUCs) interpolate baseband signals to 128 MS/s before translating them to the selected output frequency. The DDCs and DUCs combined with the high sample rates also greatly simplify analog filtering requirements. Daughterboards mounted on the USRP provide flexible, fully integrated RF front-ends. A wide variety of available daughterboards allows the use of different frequencies for a broad range of applications. The USRP accommodates up to two RF transceiver daughterboards (or two transmit and two receive) for RFI/O.

The features of USRP include the following:-

- (1) Four 64 MS/s 12-bit analog to digital converters,
- (2) Four 128 MS/s 14-bit digital to analog converters,
- (3) Four Digital Down-Converters with programmable decimation rates,
- (4) Two Digital Up-Converters with programmable interpolation rates,
- (5) High-speed USB 2.0 interface (480 Mb/s),
- (6) Capable of processing signals up to 16 MHz wide,
- (7) Modular architecture supports wide variety of RF daughterboards,
- (8) Auxiliary analog and digital I/O support complex radio controls such as RSSI and AGC,
- (9) Fully coherent multi-channel systems (MIMO capable) [27].

The operational principle for the experimental set-up of USRP is described as follows:

The set-up is usually carried out as shown in Figure 3.3. In the set-up, 2.4 GHz is usually chosen as the centre-frequency because of its suitability for Amateur Radio, Microwave link and Radar. Furthermore, it is a common knowledge that the

2.4 GHz band has been set aside for industrial, Scientific and Medical (ISM) purposes due to its use in microwave heating. Both transmitter and receiver are set at a height of 1 meter from the ground level. Single-tone (sinusoidal) signal is then sent from the transmitter to the receiver (which does not require modulation) and various values of the received power are obtained for

- (i) free space model,
- (ii) log-normal shadowing model, and
- (iii) two-ray ground model

for distances of 1 m, 3 m, 5 m, 7 m, 9 m, 11 m, 13 m, 15 m, 17 m and 19 m. The result is discussed in Chapter 4.

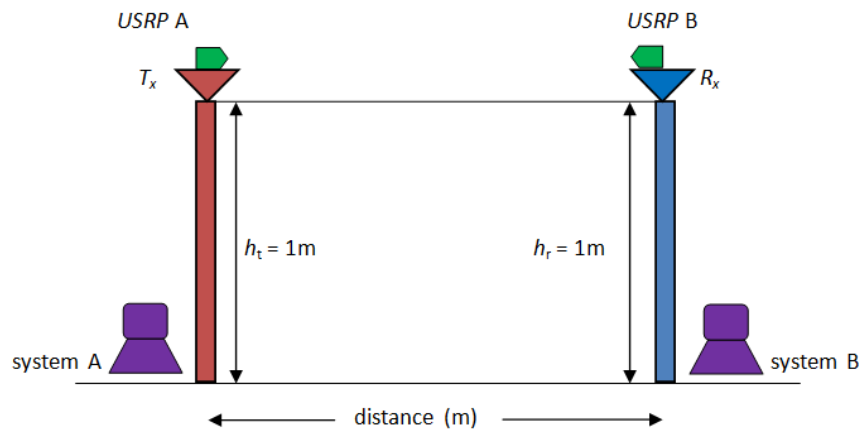


**Figure 3.3** Experimental set-up of USRP

### **3.3 Possible obstacles to localization accuracy**

Obstacles to localization accuracy of an object include environmental interferences and occlusions (e.g., the presence of liquids and metals), orientation and spatial arrangement of an object, ambient RF noise and readers' locations. These factors can weaken, scatter, or occlude radio waves, and thus lead to unreliable detection and inaccurate positioning of objects [12].

Previous techniques tend to sacrifice speed and accuracy in localizing objects in order to obtain reliable estimates. That is by carrying out repeated measurements that should consistently yield the same outcome. Unfortunately, these resulting speed and accuracy degradations tend to reduce the efficacy of the performance. However, the proposed localization framework will enable accurate object position estimation, without compromising either speed or reliability. This is because the proposed framework is highly scalable and can accommodate a wide range of requirements and tradeoffs among power, cost, accuracy and speed.

## CHAPTER 4

### SIMULATION RESULTS AND ANALYSIS

#### 4.1 Simulation Set-up

The Simulation of this work was carried out in Matlab environment [28]. The simulation results are hereby presented in this Chapter. Furthermore, each presented result is analyzed for the sake clarity.

First, Equation (2.34) was simulated in order to observe the graphical relation between phase-difference and distance. Figure 4.1 was obtained in the process, which shows that the range is directly proportional to the phase difference between two signals emanating from the transmitter.



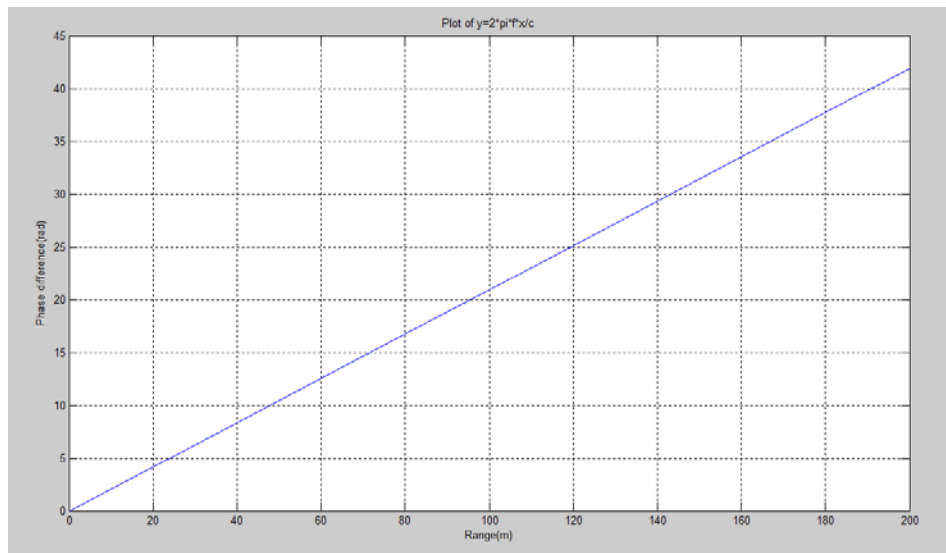


**Figure 4.1** Phase Difference Vs. Distance Relation

Next, the simulation was set-up, to obtain the Dual-frequency estimator results. Here, two pairs of operating frequencies were used with the following parameters:

Center frequency,  $f_c = 2.4$  GHz,

$$\text{Lower frequency, } f_1 = f_c - \frac{\Delta f}{2} \quad (4.1)$$

and,

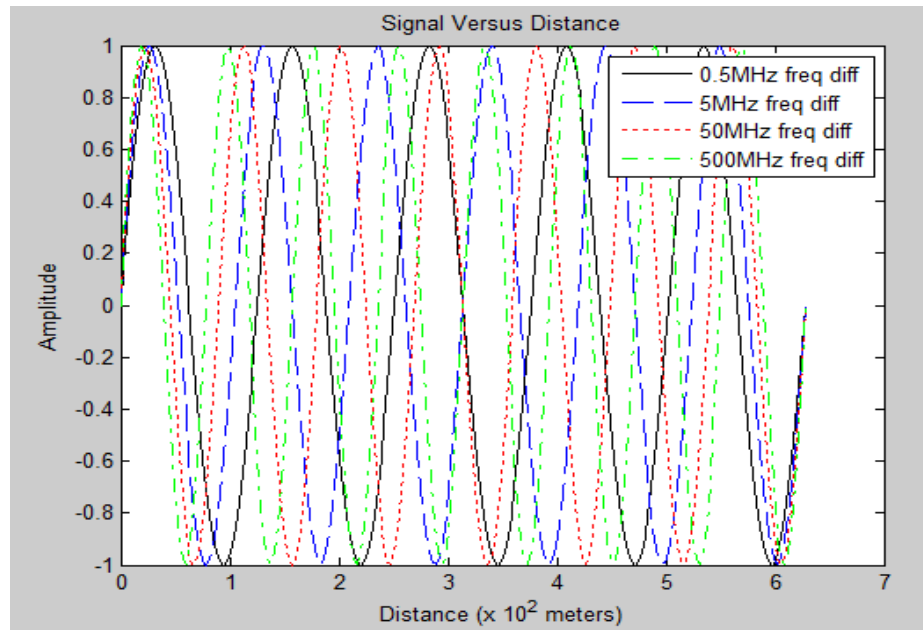
$$\text{Upper frequency, } f_2 = f_c + \frac{\Delta f}{2} \quad (4.2)$$

Table 4.1 presents the results of the lower and upper frequencies, obtained for the various values of frequency difference,  $\Delta f$ .

**Table 4.1** The operating frequencies used for Simulation

$\Delta f$ (MHz)	$f_1$ (GHz)	$f_2$ (GHz)
0.5	2.39975	2.40025
5	2.3975	2.4025
50	2.375	2.425
500	2.15	2.65

These frequencies different selections were evaluated in terms of phase difference for range cover, up till 600 meters [3]. The dual-frequency estimator results in Figure 4.2 were obtained.



**Figure 4.2** Dual-frequency Estimator results

It could be seen from Figure 4.2 that with centre-frequency  $f_c$  at 2.4 GHz, five different levels of frequency difference run on the Matlab produced varying sinusoids, each having different impact on the required range.

Further, the simulation set-up was carried out for the various propagation models as follows:

## 4.2 Propagation models simulation results

Equations (2.11), (2.12) and (2.14) were simulated in Matlab environment for the Two-ray model, Log-normal Shadowing model and Free-space model respectively. Furthermore, experimental set-up was carried out to see signal propagation using USRP as well. Received power were read at distances 1 m, 3 m, 5 m, 7 m, 9 m, 11 m, 13 m, 15 m, 17 m and 19 m. The simulation results are as shown in Figure 4.3.

It could be seen from the results of Figure 4.3 that the free-space propagation model is close to the USRP result. This shows the acceptability and reliability of free-space model in the one-way short-range propagation scenario.

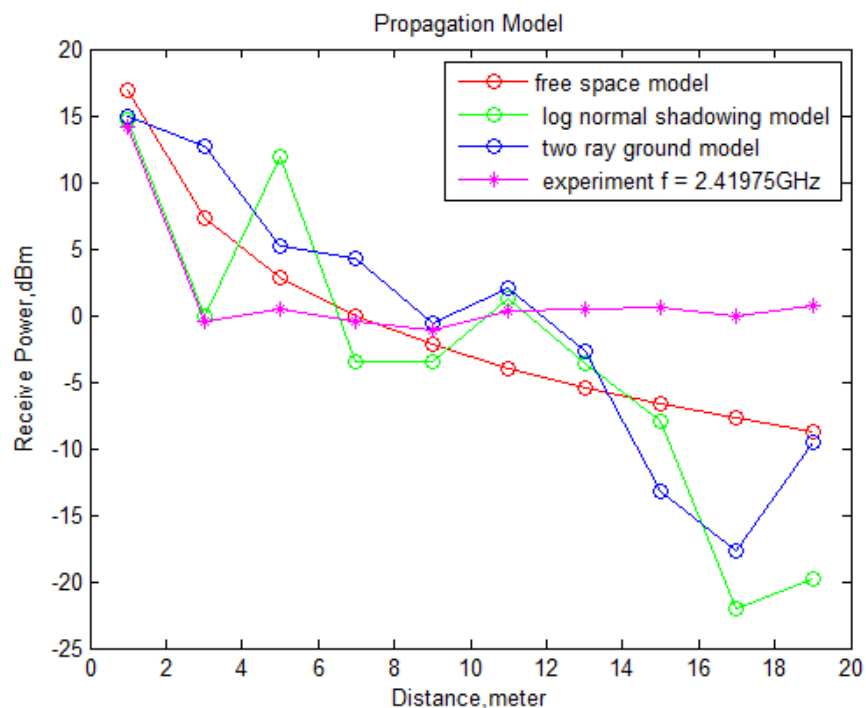


**Figure 4.3** Propagation models graphs

The result analysis is further carried out via range ambiguity, the effect of noise and error analysis in the following subsections.

### 4.3 Range ambiguity

The equation which generates the phase difference of two signals with different frequencies is obtained as follows:

$$\Delta\theta = \varphi_{0f_i} + \Delta\omega t + \phi_{nf_i} \quad (4.3)$$

where,

$$\Delta\omega = 2\pi(f_2 - f_1) \quad (4.4)$$

$$\therefore \Delta\theta = (\varphi_{0f_2} + 2\pi f_2 t + \phi_{nf_2}) - (\varphi_{0f_1} + 2\pi f_1 t + \phi_{nf_1}) \quad (4.5)$$

where  $\varphi_{0f_i}$  is the phase for each frequency carrier, and

$\phi_{nf_i}$  is the phase noise generated using normally distributed noise with variance of  $15^0$  which use to exist in a practical scenario [3].

Now, on the issue of the range ambiguity which was being introduced into the system by the second term in Equation (2.33). Figure 4.4 shows that for a particular phase difference  $\Delta\phi(t)$ , there could be infinite values of range estimate  $R(t)$ , separated from each other by  $\frac{c(m-n)}{\Delta f}$ .

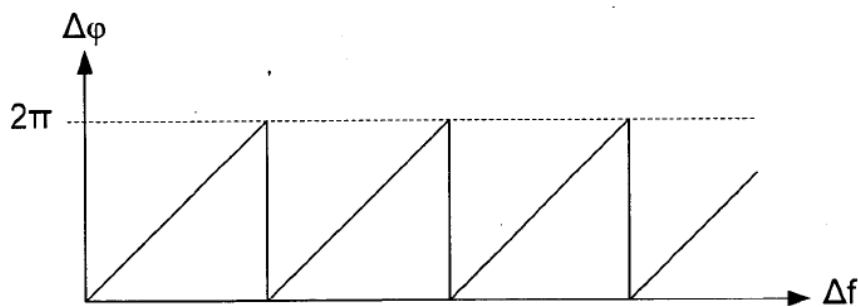


**Figure 4.4** Range ambiguity analysis

In Equation (2.33),  $m$  and  $n$  are the complete cycle values of the travelling signal that arrived at the receiver. These values are difficult to estimate in real world applications [3]. However, if the value of  $\Delta f$  is small enough, then Equations (2.29) and (2.30) will almost be just one and same equation, implying that the value of  $m$  is almost equal to the value of  $n$ . Hence, the second term in Equation (2.33) can be ignored.

Therefore, Range ambiguity situation which tends to occur when there is considerable number of frequency separations for the same phase-difference, could be eradicated by ensuring proper selection of the frequency difference  $\Delta f$  which will guarantee that the value of  $m$  is almost equal to the value of  $n$  [3].

It was therefore noted in Figure 4.2 that frequency separations of  $0.5\text{ MHz}$ ,  $5\text{ MHz}$  and  $50\text{ MHz}$  were suitable to take care of range ambiguity. For these separations, the values of  $m$  and  $n$  were almost equal. For higher frequency separations, the difference in  $m$  and  $n$  began to exist, which can no longer be ignored.

However, phase ambiguity exists since the value of phase can only be measured in the range of  $[-\pi, \pi]$  [3]. This is shown in Figure 4.5, as phase difference changes over time and time is related to distance.

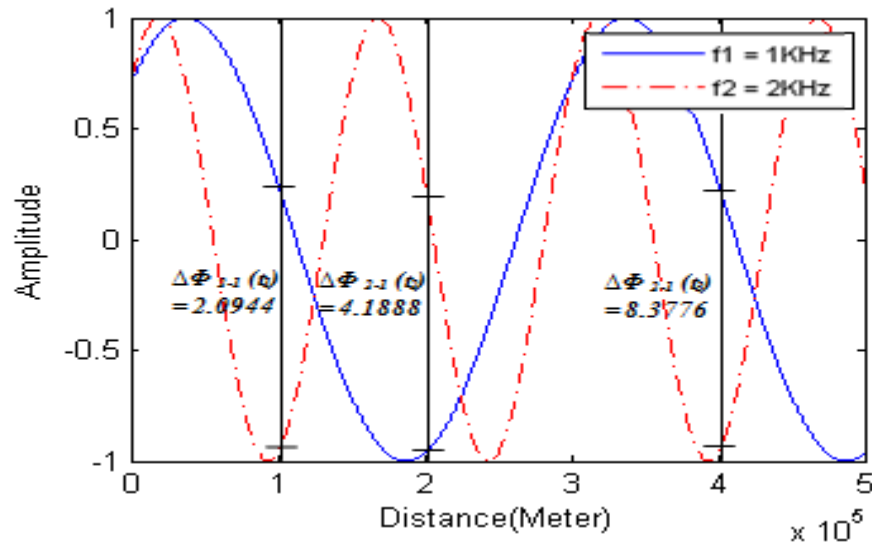


**Figure 4.5** Phase difference of two signals with time

#### 4.4 Effect of Phase Noise

Noise is a term generally used to refer to any spurious or undesired disturbances that mask the received signal in a communication system. Noise, in a communication system, is otherwise referred to Interference.

Phase noise is the result of small random fluctuations or uncertainty in the phase of an electronic signal. Such interference was therefore introduced into the

phase of the transmitted signal and sent together with the wanted signal, in order understudy its effect on the propagation scenario via ranging estimation.

Figure 4.6 presents the simulated graphs obtained for various frequency-differences of 10MHz, 1MHz and 0.5MHz, for both ‘Noisy’ signals and ‘No-noise’ signals.

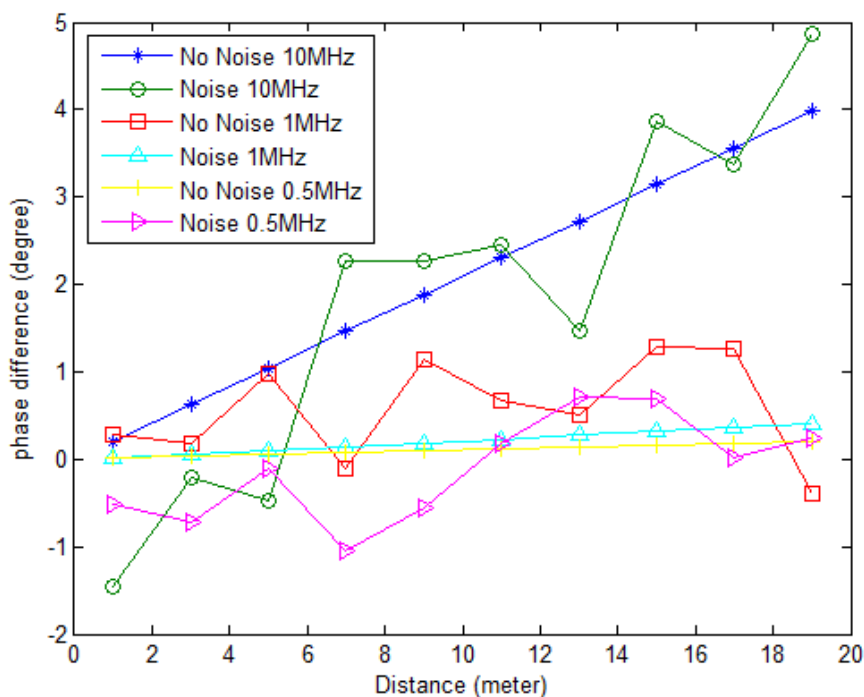


**Figure 4.6** Effect of phase noise on the signal propagation

From Figure 4.6, it could be seen that at No-noise,  
for 10 MHz,

$$\begin{aligned}\Delta d &= (9 - 5) \text{ meters} \\ &= 4 \text{ meters}\end{aligned}$$

and

$$\begin{aligned}\Delta\phi(t) &= (2-1)^0 \\ &= 1^0\end{aligned}$$

Therefore, if  $1^0$  corresponds to 4 meters,  
then,  $15^0$  would correspond to  $(4 \times 15)$  meters = 60 meters.

Secondly,  
for 1 *MHz*,

$$\begin{aligned}\Delta d &= (11-1)\text{meters} \\ &= 10\text{meters}\end{aligned}$$

and

$$\Delta\phi(t) = 0.2^0$$

Therefore, if  $0.2^0$  corresponds to 10 meters,  
then,  $15^0$  would correspond to  $\frac{10}{0.2} \times 15$  meters = 750 meters.

Also,  
for 0.5 *MHz*,

$$\begin{aligned}\Delta d &= (19-1)\text{meters} \\ &= 18\text{meters}\end{aligned}$$

and

$$\Delta\phi(t) = 0.2^0$$

Therefore, if  $0.2^0$  corresponds to 18 meters,  
then,  $15^0$  would correspond to  $\frac{18}{0.2} \times 15$  meters = 1350 meters.



Furthermore, Figure 4.7 shows the plot of values of phase difference with corresponding values of distance from 1 meter to 500 meters.

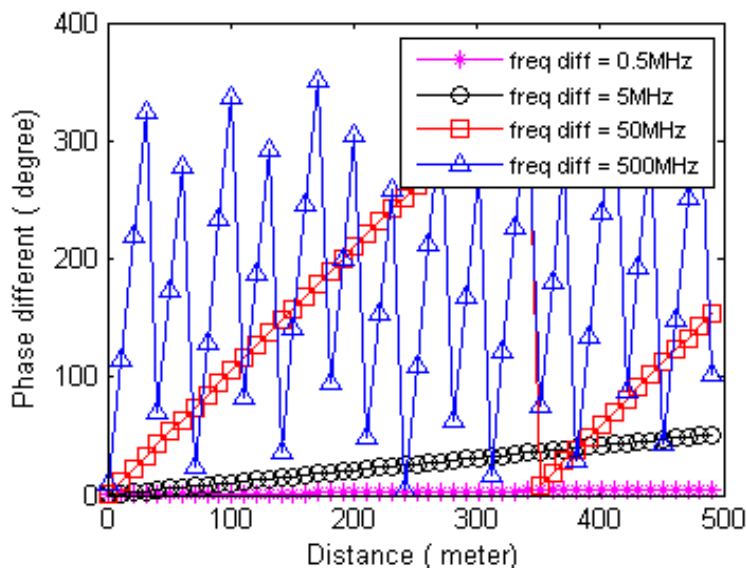


**Figure 4.7** Phase difference over 500 meters

It could be seen from Figure 4.7 that  $\Delta\phi(t)$  is not identical to each other for smaller values of  $\Delta f$ . Specifically, for  $\Delta f = 0.5 \text{ MHz}$  and  $\Delta f = 5 \text{ MHz}$ , suitability is guaranteed for the propagation within 500 meters. Frequency difference of  $\Delta f = 50 \text{ MHz}$ , is suitable within 100 meters. For higher frequency difference,  $\Delta\phi(t)$  is easily affected by noise. This is because the proportionality between the phase difference and distance is not direct unlike in the case of the lower frequency difference. This further confirms that lower values of  $\Delta f$  are suitable for short-range application since the value of  $\Delta\phi(t)$  will not vary much from the real expected value [3].

## 4.5 Error Analysis

The errors were analyzed via distance error and phase error. Table 4.2 presents the obtained results, the simulation of which produced Figure 4.8.

**Table 4.2** Distance error Vs Phase error

Phase error ( $^{\circ}$ )	Distance error(m)
0.001	2.5
0.005	2.5
0.01	2.5
0.05	2.5
0.1	2.8
0.5	5
1	10
5	25
10	50
50	240

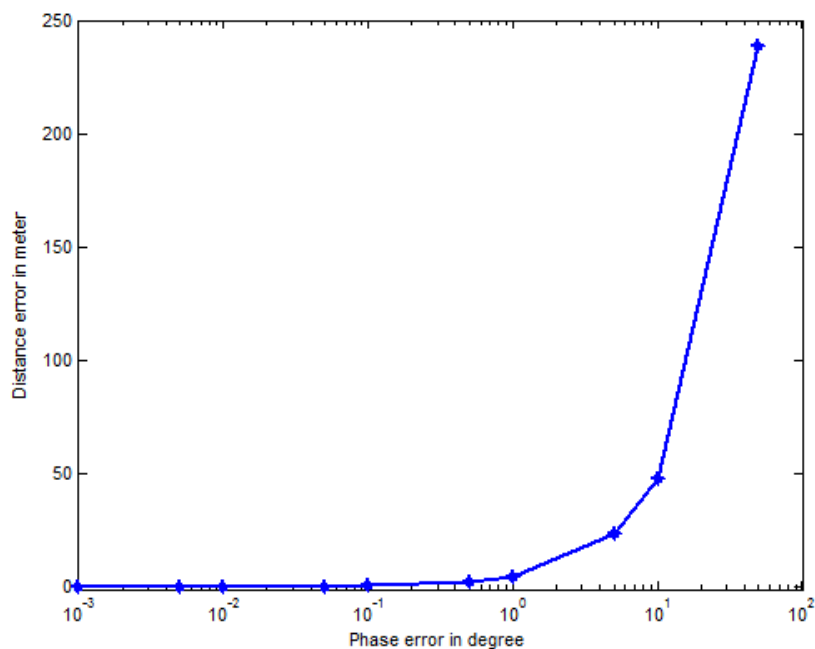


**Figure 4.8** Distance error Vs Phase error graph

It could be deduced from the graph of Figure 4.8 that the employed dual-frequency technique for range estimation is very suitable for short range application of within 100 meters (corresponding to  $15^0$  phase error) at lower frequency separations of up to 50 *MHz*.

## **CHAPTER 5**

### **CONCLUSION**

#### **5.1 Introduction**

This chapter concludes the project development through a re-cap of the objectives set out for this work, the simulated results and analysis, and recommendations are offered for future improvement of Ranging estimation.

#### **5.2 Conclusion**

In this work, the employed dual-frequency technique provides the capability of estimating the range of objects over a short-range application. This is because Range estimation is important to providing localization and tracking of assets and objects in various applications. The objectives set for this work were achieved through:

- (i) adequate understudying the signal propagation via free-space propagation model, log-normal propagation model and two-ray propagation model,
- (ii) carrying out simulations in Matlab environment; results being presented in Chapter 4,
- (iii) analyzing the range ambiguity and effect of noise on the range estimation, also in Chapter 4.

The basic concept introduced in this dual-frequency ranging technique is that when two different signals travel from a transmitter  $T_x$  and arrive at the receiver  $R_x$ , the phase difference between these two signals at the receiver can be used to estimate the distance between the transmitter and the receiver.

As discussed in sections 4.3 and 4.4, the phase difference,  $\Delta\phi(t)$  has direct relation with the frequency difference,  $\Delta f$ , which must not be too high in order to avoid range ambiguity, and to drastically reduce the influence of noise on the result.

From the simulations results therefore, lower frequency difference of up to 50  $MHz$  is very suitable for short-range ranging estimation application of within 100 meters.

### **5.3 Recommendation for Future work**

Having achieved the objectives set out for this work, there is however, room for further improvement. This is because of the enormous importance which the

subject of range estimation offers in the propagation environment in particular and communication industry in general. The following recommendations are therefore humbly made.

(i) It is recommended that the work be carried out as well for a long-range application in a multipath environment.

(ii) Field measurement is recommended to be done using USRP, and the results be compared with the Matlab simulated results.

(iii) The effect of synchronization is also recommended for investigation in a non line-of-sight propagation environment.

## REFERENCES

1. Suzhe, W. and Yong, L. Node localization algorithm based on RSSI in wireless sensor network. *Signal Processing and Communication System (ICSPCS), 2012. 6<sup>th</sup> International Conference.* IEEE, 2012.
2. Shi, Q., Correal, N., Kyperountas, S., and Niu, F. (2005). Performance comparison between TOA ranging technologies and RSSI ranging technologies for multi-hop wireless networks. In *Vehicular Technology Conference, 2005. VTC-2005-Fall. 2005 IEEE 62nd* (Vol. 1, pp. 434-438). IEEE.
3. Hassan, N. A. C., Yusof, K. M., and Yusof, S. K. S. (2015, August). Ranging Estimation Using Dual-Frequency Doppler Technique. In *IT Convergence and Security (ICITCS), 2015 5th International Conference on* (pp. 1-5). IEEE.
4. Barsocchi, P., Lenzi, S., Chessa, S., and Giunta, G. (2009, April). A novel approach to indoor RSSI localization by automatic calibration of the wireless propagation model. In *Vehicular Technology Conference, 2009. VTC Spring 2009. IEEE 69th* (pp. 1-5). IEEE.

5. Scherhaufel, M., Pichler, M., Muller, D., Ziroff, A. and Stelzer, A. Phase-of-arrival-based localization of passive UHF RFID tags. *Microwave Symposium Digest (IMS), 2013 IEEE MTT-S International*. IEEE, 2013.
6. Andreas, P, Miesen, R, and Vossiek, M. Inverse sar-approach for localization of moving rfid tags. *RFID (RFID), 2013 IEEE International Conference on*. IEEE, 2013.
7. Ahmad, F., Amin, M. G., and Zeman, P. D. (2009). Dual-frequency radars for target localization in urban sensing. *IEEE transactions on aerospace and electronic systems*, 45(4), 1598-1609.
8. Armoogum, V., Soyjaudah, K. M. S., Mohamudally, N., and Fogarty, T. (2007, May). Comparative study of path loss using existing models for digital television broadcasting for summer season in the north of mauritius. In *Telecommunications, 2007. AICT 2007. The Third Advanced International Conference on* (pp. 34-34). IEEE.
9. Rachelin, S. P. and Saravanan, T. Target Tracking in Wireless Sensor Networks Using ICTP and Miss Mechanism. *Middle-East Journal of Scientific Research* vol. 20, no.12. 2014.
10. Mustafa, M. Y., Eilertsen, S. M., Hansen, I., Pettersen, E., and Kronen, A. (2013, March). Matching mother and calf reindeer using wireless sensor networks. In *Computer Science and Information Technology (CSIT), 2013 5th International Conference on* (pp. 99-105). IEEE.
11. Hekmat, R. (2006). Modeling Ad-hoc Networks. *Ad-hoc Networks: Fundamental Properties and Network Topologies*, 15-39.



12. Lu, Y., Zhang, W., Meng, Y., and Yu, H. (2011, December). A novel approach for accurately and quickly localizing a tag from a mass of passive RFID tags. In *Intelligent Sensors, Sensor Networks and Information Processing (ISSNIP), 2011 Seventh International Conference on* (pp. 485-489). IEEE.
13. Bouet, M. and Aldri, L. D. S. RFID tags: Positioning principles and localization techniques. *Wireless Days, 2008. WD'08. 1st IFIP*. IEEE, 2008.
14. Mao, G., Fidan, B. and Anderson, B. D. Wireless sensor network localization techniques. *Computer networks*, vol. 51, no. 10. 2007.
15. Oguejiofor, O., Aniedu, A., Ejiofor, H. and Okolibe, A. Trilateration based localization algorithm for wireless sensor network. *International Journal of Science Mod. Engineering*, vol. 97, no. 2. 2009.
16. Zhang, Y., Amin, M., and Ahmad, F. (2007, November). A novel approach for multiple moving target localization using dual-frequency radars and time-frequency distributions. In *Signals, Systems and Computers, 2007. ACSSC 2007. Conference Record of the Forty-First Asilomar Conference on* (pp. 1817-1821). IEEE.
17. Tan, D. K. P., Lesturgie, M., Sun, H. and Lu, Y. Moving target localization using dual-frequency continuous wave radar for urban sensing applications. *Radar Conference-Surveillance for a Safer World, 2009. RADAR. International*. IEEE, 2009.
18. Wang, L., Argumedo, A., and Washington, W. (2014). Precise asymptotic distribution of the number of isolated nodes in wireless networks with lognormal shadowing. *Applied Mathematics*, 5(15), 2249.

19. Cheng, L., Wu, C., Zhang, Y., Wu, H., Li, M., and Maple, C. (2012). A survey of localization in wireless sensor network. *International Journal of Distributed Sensor Networks*, 2012.
20. Shang, J., Yu, S., and Zhu, L. (2009, January). Location-aware systems for short-range wireless networks. In *Computer Network and Multimedia Technology, 2009. CNMT 2009. International Symposium on* (pp. 1-5). IEEE.
21. Maroti, M., Volgyesi, P., Dora, S., Kusy, B., Nadas, A., Ledeczi, A., Balogh, G. and Molnar, K. Radio interferometric geolocation. *Proceedings of the 3rd international conference on Embedded networked sensor systems*. ACM, 2005.
22. Bölcskei, H. (2001). Blind estimation of symbol timing and carrier frequency offset in wireless OFDM systems. *Communications, IEEE Transactions on*, 49(6), 988-999.
23. Zhang, Y., Amin, M., and Ahmad, F. (2008). Time-frequency analysis for the localization of multiple moving targets using dual-frequency radars. *Signal Processing Letters, IEEE*, 15, 777-780.
24. Yusof, K. M. and Fitz, S. Short range frequency estimation for localization in cognitive radio environment. *International Conference on Computer Communication Networks, ICCCN 2011*. IEEE, 2011.
25. Ahmad, F., Amin, M. G. and Zeman, P. D. Performance analysis of dual-frequency CW radars for motion detection and ranging in urban sensing

- applications. *Defense and Security Symposium*. International Society for Optics and Photonics, 2007.
26. Akiyama, T., Nakamura, M., Sugimoto, M. and Hashizume, H. Smart phone localization method using dual-carrier acoustic waves. *Indoor Positioning and Indoor Navigation (IPIN), 2013 International Conference*. IEEE, 2013.
  27. Kambiz, S., Soltan, M. and Moshfeghi, M. Method and system for determining the distance between an RFID reader and an RFID tag using phase. U.S. Patent Application 11/641,623. 2006.
  28. Leong, K. S., Ng, M. L., and Cole, P. H. (2006, January). Positioning analysis of multiple antennas in a dense RFID reader environment. In *Applications and the Internet Workshops, 2006. SAINT Workshops 2006. International Symposium on* (pp. 4-pp). IEEE.

## APPENDICES

**APPENDIX A****RANGE VERSUS PHASE-DIFFERENCE CODE**

```
x=0:20:200;  
y=2*pi*10*10^6*x/(3*10^8);  
plot(x,y);  
title('Plot of  $y=2\pi f x/c$ ');  
xlabel('Range(m)');  
ylabel('Phase difference(rad)');  
grid on;
```

## APPENDIX B

### CODE FOR THE EFFECT OF NOISE ON SIGNAL PROPAGATION

```

f1 = 2.4e9 - 5e6;
f2 = 2.4e9 + 5e6;
f3 = 2.4e9 - 0.5e6;
f4 = 2.4e9 + 0.5e6;
f5 = 2.4e9 - 0.25e6;
f6 = 2.4e9 + 0.25e6;
D = 1:2:20;
C = 3*10^8;
time = D / C ;
%niadalah phase of the signal tanpa noise.
P12 = ((2*pi*f2)-(2*pi*f1))*time; % phase difference of 2 freq10Mhz
P34 = ((2*pi*f4)-(2*pi*f3))*time; % 1MHz
P56 = ((2*pi*f6)-(2*pi*f5))*time; %0.5MHz
sz = size(time);
theta1n1 = (2*pi*f1*time) + (sqrt((15/180)*pi))*randn(sz) + mean(P12);

theta2n1 = (2*pi*f2*time) + (sqrt((15/180)*pi))*randn(sz) + mean(P12);
P12_noise = theta2n1 - theta1n1;

```

```

theta1n2 = (2*pi*f3*time) + (sqrt((15/180)*pi))*randn(sz) + mean(P34);
theta2n2 = (2*pi*f4*time) + (sqrt((15/180)*pi))*randn(sz) + mean(P34);
P12_noise1 = theta2n2 - theta1n2;
theta1n3 = (2*pi*f5*time) + (sqrt((15/180)*pi))*randn(sz) + mean(P56);
theta3n1 = (2*pi*f6*time) + (sqrt((15/180)*pi))*randn(sz) + mean(P56);
P12_noise2 = theta3n1 - theta1n3;
d12 = 2*pi*(f2-f1);
d21 = C / d12;
df_noise = (d21* P12_noise);
de_noise = D - df_noise;
d34 = 2*pi*(f4-f3);
d43 = C / d34;
df_noise1 = (d43* P12_noise1);
de_noise1 = D - df_noise1;
d56 = 2*pi*(f4-f3);
d65 = C / d56;
df_noise2 = (d65* P12_noise2);
de_noise2 = D - df_noise2;
figure
set(gcf,'color','white')
plot (D,P12,'-*',D,P12_noise,'-o',D,P12_noise1,'-rs',D,P34,'k-^',D,P56,'y-
+',D,P12_noise2,'g->')
legend('No Noise 10MHz','Noise 10MHz','No Noise 1MHz','Noise
1MHz','No Noise 0.5MHz','Noise 0.5MHz','location','northwest')
xlabel('Distance (meter)')
ylabel('phase difference (degree)')
%ylim([-2 2])
figure
set(gcf,'color','white')
plot (D,de_noise,'-o',D,de_noise1,'-rs',D,de_noise2,'-^')

```

```
legend('Noise 10MHz','Noise 1MHz','Noise 0.5MHz','location','southeast')  
xlabel('Distance (meter)')  
ylabel('error (meter)')  
grid on
```

## APPENDIX C

### DISTANCE ERROR VERSUS PHASE ERROR CODE

```

a = [3 5 6 9 12 15 18 21 24 27 30]; % no of sample
b = [0.504451366 0.362985993 0.238900961 0.161617728 0.139045787
0.133009991 0.125743177 0.110583847 0.098528411 0.112143764
0.115902647]; %rmsemle
c = [0.337411172 0.277563097 0.404998642 0.433410245 0.450832963
0.461374771 0.467663081 0.472027563 0.476732891 0.479692366
0.482266363]; %rmselse
d = [0.742884929 0.839563265 2.542814286 0 5.206404177 12.1570605
14.58707658 16.20275377 23.5151271 25.29466008 25.17918633];
%rmsecrt
figure
set(gcf,'color','white')
set(0, 'DefaultAxesFontSize', 8, 'DefaultAxesFontName','Arial');
% set(0,'DefaultAxesLineStyleOrder',{'-',':','--'})
% figure;
set(gcf, 'Units', 'centimeter');
pos = get(gcf, 'Position');
pos(3) = 10; % figure box size 9.7cm x 6.3cm

```



```

pos(4) = 7.5; % default 6.3
set(gcf, 'Position', pos);
set(gca, 'Units', 'centimeter');
set(gca, 'Position', [1.3 0.9 8 5]); %axes box size 8cm x 5cm
subplot(3,1,1)
plot(a,b,'-*b')
legend('MLE')
ylabel('RMSE')
xlim([2 31])
ylim([0 0.6])
subplot(3,1,2)
plot(a,c,'-or')
legend('LSE')
ylabel('RMSE')
xlim([2 31])
ylim([0.1 0.6])
subplot(3,1,3)
plot(a,d,'-+g')
ylim([-3 27])
xlim([2 31])
legend('CRT')
xlabel('sample')
ylabel('RMSE')
a = [0.20943951 0.628318531 1.047197551 1.466076572 1.884955592
2.303834613 2.722713633 3.141592654 3.560471674 3.979350695]; % real
phase
b = [0.2736 0.7914 0.9894 2.1336 2.5006 1.9921 2.6728 3.0596 3.7129
4.5532]; % estimate phase mle
c = [0.187833319 0.652675043 1.1317 2.012061032 2.361914555 2.1975769
2.857003533 3.25493212 3.377071674 4.380370948]; % estimate phase lse

```

```

d = [0.1951 0.6125 0.1504 0.9405 1.793 1.9552 0.9256 2.6312 3.2301
2.4832]; % estimate phase crt
figure
set(gcf,'color','white')
set (0, 'DefaultAxesFontSize', 8, 'DefaultAxesFontName','Arial');
% set (0,'DefaultAxesLineStyleOrder',{'-',':','--'})
% figure;
set (gcf, 'Units', 'centimeter');
pos = get (gcf, 'Position');
pos(3) = 10; % figure box size 9.7cm x 6.3cm
pos(4) = 7.5; % default 6.3
set (gcf, 'Position', pos);
set (gca, 'Units', 'centimeter');
set (gca, 'Position', [1.3 0.9 8 5]); %axes box size 8cm x 5cm
plot (a,a,'-k',a,b,'-*b',a,c,'-or',a,d,'-+g')
ylim ([0 4.7])
xlim ([0.1 4.1])
legend ('Actual Phase','MLE','LSE','CRT')
xlabel('Real Phase in degree')
ylabel('Estimate Phase in degree')
title('Estimate Phase vs Real Phase')
a = [1 3 5 7 9 11 13 15 17 19]; %real distance
b = [1.306343773 3.778656659 4.724037021 10.1871896 11.93948552
9.511576864 12.76167996 14.60851392 17.72779165 21.73992861]; %
estimate distance mle
c = [0.896838036 3.11629378 5.403469473 9.606883771 11.2773113
10.49265679 13.64118704 15.54115609 16.1243295 20.91473067]; %
estimate distance lse
d = [0.931533882 2.924472079 0.718107103 4.49E+00 8.560944389

```

```

9.335392342 4.41941446 12.56305459 15.42259145 11.85640664]; %
estimate distance crt
figure
set(gcf,'color','white')
set (0, 'DefaultAxesFontSize', 8, 'DefaultAxesFontName','Arial');

% set (0,'DefaultAxesLineStyleOrder',{'-',':','--'})
% figure;
set (gcf, 'Units', 'centimeter');
pos = get (gcf, 'Position');
pos(3) = 10; % figure box size 9.7cm x 6.3cm
pos(4) = 7.5; % default 6.3
set (gcf, 'Position', pos);
set (gca, 'Units', 'centimeter');
set (gca, 'Position', [1.3 0.9 8 5]); %axes box size 8cm x 5cm
plot (a,a,'-k',a,b,'-*b',a,c,'-or',a,d,'-+g')
ylim ([0.5 22])
xlim ([0.5 19.5])
legend ('Actual Distance','MLE','LSE','CRT')
xlabel('Actual Distance in meter')
ylabel('Estimate Distance in meter')
title('Estimate Distance vs Real Distance')
a = [0.001 0.005 0.01 0.05 0.1 0.5 1 5 10 50]; % phase error
b = [0.004774648 0.023873241 0.047746483 0.238732415 0.477464829
2.387324146 4.774648293 23.87324146 47.74648293 238.7324146]; %
Distance error
figure
set(gcf,'color','white')
semilogx(a,b,'-*','LineWidth',2)
ylim ([-1 250])

```

```

xlabel('Phase error in degree')
ylabel('Distance error in meter')
a = [1 2 3 4 5 6 7 8 9 10 11 12 13 14 15 16 17 18 19 20 21 22 23 24 25 26 27
28 29 30 31 32 33 34 35 36 37 38 39 40 41 42 43 44 45]; % phase error
b=[4.77464829275686,9.54929658551372,14.3239448782706,19.098593171
0274,23.8732414637843,28.6478897565412,33.4225380492980,38.1971863
420549,42.9718346348117,47.7464829275686,52.5211312203255,57.29577
95130823,62.0704278058392,66.8450760985960,71.6197243913529,76.394
3726841098,81.1690209768666,85.9436692696235,90.7183175623803,95.4
929658551372,100.267614147894,105.042262440651,109.816910733408,11
4.591559026165,119.366207318921,124.140855611678,128.915503904435,
133.690152197192,138.464800489949,143.239448782706,148.01409707546
3,152.788745368220,157.563393660976,162.338041953733,167.112690246
490,171.887338539247,176.661986832004,181.436635124761,186.2112834
17518,190.985931710274,195.760580003031,200.535228295788,205.30987
6588545,210.084524881302,214.859173174059]; % Distance error
figure
set(gcf,'color','white')
set(0, 'DefaultAxesFontSize', 8, 'DefaultAxesFontName','Arial');
% set(0,'DefaultAxesLineStyleOrder',{'-',':','--'})
% figure;
set(gcf, 'Units', 'centimeter');
pos = get(gcf, 'Position');
pos(3) = 10; % figure box size 9.7cm x 6.3cm
pos(4) = 7.5; % default 6.3
set(gcf, 'Position', pos);
set(gca, 'Units', 'centimeter');
set(gca, 'Position', [1.3 0.9 8 5]); %axes box size 8cm x 5cm
plot(a,b,'m-^')
%ylim ([-1 250])

```

```
xlabel('Phase error in degree')  
ylabel('Distance error in meter')  
legend ('Distance = 15m')  
xlim ([0 47])  
title('Distance Error vs Phase Error')
```